JOURNAL OF THERMOPHYSICS AND HEAT TRANSFER
Vol. 24, No. 2, April–June 2010

Nonsteady Effective Thermal Conductivity of Dense Fibrous Composites with Graded Interface

Xue-Qian Fang* and Xiao-Hua Wang†
Shijiazhuang Railway Institute, 050043 Shijiazhuang, People's Republic of China
Chao Hu‡
Tongji University, 200092 Shanghai, People's Republic of China
and
Wen-Hu Huang§
Harbin Institute of Technology, 150001 Harbin, People's Republic of China

DOI: 10.2514/1.45295

The multiple scattering of thermal waves by dense fibers with a functionally graded interface in composites is considered, and the analytical solution of the nonsteady effective thermal conductivity of composites is presented. The Fourier heat conduction law is applied to analyze the propagation of thermal waves in the fibrous composite. The scattering and refraction of thermal waves by cylindrical fibers with a nonhomogeneous interface layer in the matrix are expressed by using the wave function expansion method. The theory of quasi-crystalline approximation and the conditional probability density function are employed to treat the multiple scattering of thermal waves from the dense fibers. Through analysis, it is found that the nonsteady effective thermal conductivity under higher frequencies is quite different from the steady thermal conductivity. In different regions of wave frequency, the effects of the functional form of gradation and the properties and thickness of the functionally graded layers on the nonsteady effective thermal conductivity show great differences.

I. Introduction

THE subject of the effective thermal conductivity of composites is one of the classical problems in heterogeneous media that has recently received renewed interest due to the increasing importance of high-temperature systems, e.g., car manufacturing, dedicated space structures, etc. These materials usually undergo a complex thermal history. Determining the effective thermal properties of composites is crucial for a successful design and for the manufacture of materials. The development of micromechanical models for accurately predicting the effective thermal conductivity of multiphase composites has been the specific objective to study.

The methods used to measure the thermal conductivity of composites are divided into two groups: the steady-state and the nonsteady-state methods. In the first group, the sample is subjected to a constant heat flow. In the second group, a periodic or transient heat flow is established in the sample [1]. In the past, much attention has been focused on the problems of steady state.

The earliest models for the thermal behavior of composites assumed that the two components are both homogeneous and are perfectly bounded across a sharp and distinct interface. The Maxwell solution [2] is the starting point to find the effective conductivity of two-phase material systems, but it is valid only for very low concentrations of the dispersed phase. Hasselman and Johnson [3] extended the classical work of Maxwell to consider the effects of an interfacial thermal barrier resistance in spherical particulate and cylindrical fiber-reinforced composites. Subsequently, many structural models (e.g., parallel, Maxwell–Eucken [4], and effective medium theory models [5]) were proposed. Recently, Samantray et al. [6] applied the unit-cell approach to study the effective thermal conductivity of two-phase materials. The idea of the generalized self-consistent model was also developed by Hashin and Monteiro [7] to determine the effective thermal conductivity of the two-phase materials.

Recognition of the importance of modeling the *interphase zone* in composite materials has existed for some time. Mathematical analyses of inhomogeneous interfaces probably started with the work of Kanaun and Kudriavtseva [8,9] on the effective elasticity of a medium with spherical inclusions surrounded by radially inhomogeneous interphase zones. Subsequently, Lutz and Ferrari [10] considered the effective bulk modulus of composites reinforced by inclusions with linearly varying elastic moduli. Lutz and Zimmerman [11] considered the power law variation in the context of effective bulk modulus and effective conductivity. Recently, Taguchi et al. [12] investigated the effect of these interphase layers on the microstructure, mechanical, and thermal properties of SiC/SiC composites. Sevostianov and Kachanov [13] analyzed the effect of interface layers on the overall elastic/conductive properties of composites with nanoparticles.

With the wide application of composites in aerospace, automotive industries, and other high-temperature situations, a functionally graded interface between the fibers and the matrix has been introduced in the design of composites to minimize thermal stresses and enhance thermal properties. In high-temperature situations, the solving method in the steady state becomes inaccurate. The nonsteady-state method is an efficient way of predicting the effective thermal conductivity of composites under high-temperature situations. Recently, Monde and Mitsutake [14] proposed a method for determining the thermal conductivity of solids by using an analytical inverse solution for unsteady heat conduction. By using modulated photothermal techniques, Salazar et al. [1] studied the effective thermal conductivity of composites made of a matrix filled with aligned circular cylinders of a different material. In a series of works by Fang et al., photothermal method was applied to investigate the effects of coating on the nonsteady effective thermal conductivity of fibrous [15] and particular composites [16]. Recently, Fang [17] employed the thermal wave method and the theory of Waterman and Truell [18] to study the effect of the functionally graded interface on the nonsteady effective thermal conductivity of fibrous composites.

Received 5 May 2009; revision received 31 October 2009; accepted for publication 3 November 2009.

*Department of Engineering Mechanics; fangxueqian@163.com (Corresponding Author).
†School of Computing and Informatics.
‡School of Aerospace Engineering and Applied Mechanics.
§Department of Aerospace Engineering and Mechanics.

However, this theory neglects the multiple scattering effects among the fibers and is only suited to dilute concentrations of fibers.

The main objective of this paper is to extend the work of Fang [17] to the multiple scattering of thermal waves by the dense fibers with a functionally graded interface in composites, and the effects of the interface on the nonsteady effective thermal conductivity of composites are analyzed. The composite medium contains a random distribution of cylindrical inclusions of the same size with interface layers of the same thickness. The interface layer is modeled by any number of homogeneous layers. The temperature fields in different regions of composites are expressed by using the wave function expansion method, and the expanded mode coefficients are determined by satisfying the boundary conditions at the interfaces. Considering that the positions of the fibers are random, the temperature fields in composites are averaged. The averaged equations are solved by using Lax's quasi-crystalline approximation [19], and the effective propagating wave number and the nonsteady effective thermal conductivity of composites are obtained.

II. Formulation of the Problem

Consider a composite material containing a large number N of fibers embedded in an infinite matrix. The long, parallel fibers with identical properties are randomly distributed in the matrix [7,20]. As is often the case for practical fiber-reinforced composites, the matrix is assumed to be isotropic and the fibers are transversely isotropic, so the resulting unidirectional composite also possesses transverse isotropy. The fibers of radius a_0 have identical properties. Let λ, c, and ρ be the thermal conductivity, specific heat capacity, and mass density of the matrix, and let λ_0, c_0, and ρ_0 be those of the fibers. The geometry is depicted in Fig. 1, in which (x, y, z) is the Cartesian coordinate system with origin at the center of the fiber, and (r, θ, z) is the corresponding cylindrical coordinate system. The fibers are labeled by suffixes $i = 1, 2, \ldots, N$. The position vector of the center of the ith fiber is denoted by $\mathbf{r}_i$.

It is assumed that thick layers of uniform thickness h with variable material properties are present at the interfaces separating the matrix from each fiber. The interface layer is subdivided into several thin cylindrical shells, and the material properties within each shell of inner radius a_{l-1} and outer radius a_l $(l = 1, 2, \ldots, n)$ are λ_l, c_l, and ρ_l. The uniform thickness of the shells is $h_l = a_l - a_{l-1}$. Let the boundaries of the ith fiber and the shells be denoted by C_i^l $(l = 0, 1, 2, \ldots, n)$.

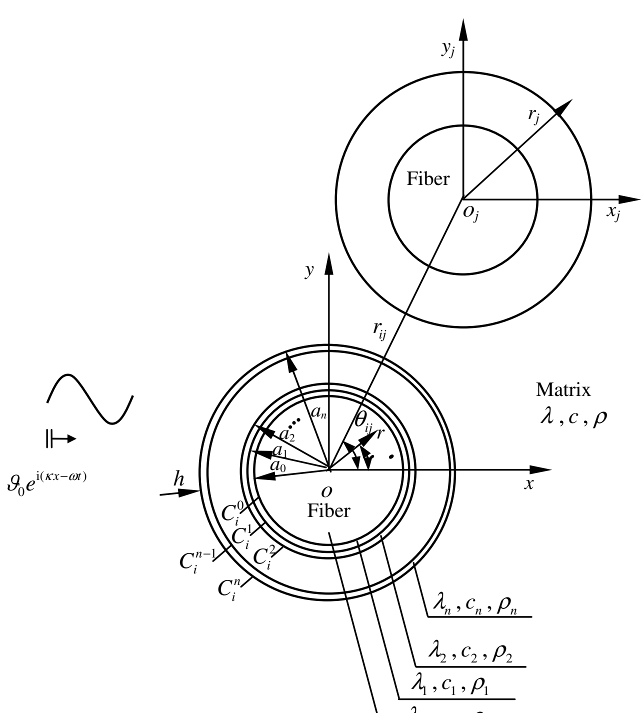

Fig. 1 Two cylindrical fibers with interface layers and wave incidence in composites.

III. Conditional Probability Density Function for Fiber Distribution

To analyze the correlation of the temperature field among the randomly distributed fibers, the conditional probability density function for fiber distribution must be specified. The probability density of the random variable $(\mathbf{r}_1, \mathbf{r}_2, \ldots, \mathbf{r}_N)$ is denoted by $p(\mathbf{r}_1, \mathbf{r}_2, \ldots, \mathbf{r}_N)$. Then, due to the indistinguishability of the cylindrical fibers, it is symmetric in its arguments, and we have

$$\begin{aligned} p(\mathbf{r}_1, \mathbf{r}_2, \ldots, \mathbf{r}_N) &= p(\mathbf{r}_i) p(\mathbf{r}_1, \mathbf{r}_2, \ldots, ', \ldots, \mathbf{r}_N | \mathbf{r}_i) \\ &= p(\mathbf{r}_i) p(\mathbf{r}_j | \mathbf{r}_i) p(\mathbf{r}_1, \mathbf{r}_2, \ldots, ', \ldots, ' \ldots, \mathbf{r}_N | \mathbf{r}_j | \mathbf{r}_i) \\ p(\mathbf{r}_i) = p(\mathbf{r}_1), \qquad & p(\mathbf{r}_j | \mathbf{r}_i) = p(\mathbf{r}_2 | \mathbf{r}_1), \qquad i \neq j \end{aligned} \tag{1}$$

where the probabilities with the vertical bar in their argument denote the customary conditional probabilities. A prime in the first part of Eq. (1) means that $\mathbf{r}_i$ is absent, and two primes in the second part of Eq. (1) mean that both $\mathbf{r}_i$ and $\mathbf{r}_j$ are absent. For a uniform composite material, the positions of a single cylindrical fiber are equally probable within a large region V of the volume of composites, and so its distribution is uniform with density; that is,

$$p(\mathbf{r}_i) = 1/V, \quad \text{if } \mathbf{r}_i \in V; \qquad p(\mathbf{r}_i) = 0, \quad \text{if } \mathbf{r}_i \notin V \tag{2}$$

If the center of the ith fiber, well within V, is held fixed, the distribution of the cylindrical fibers around it will be cylindrically symmetrical. Thus, the conditional probability density function $p(\mathbf{r}_j | \mathbf{r}_i)$ is usually expressed in terms of the pair correlation function $g(r_{ij})$; that is,

$$\begin{aligned} p(\mathbf{r}_j | \mathbf{r}_i) &= \frac{1}{V}[1 - g(r_{ij})], \quad \text{if } \mathbf{r}_j \in V \\ p(\mathbf{r}_j | \mathbf{r}_i) &= 0, \quad \text{if } \mathbf{r}_j \notin V \end{aligned} \tag{3}$$

where the pair correlation function $g(r_{ij})$ is a decreasing function of r_{ij}. The normalization condition of $p(\mathbf{r}_j | \mathbf{r}_i)$ gives, in the limit as $V \to \infty$,

$$\lim_{R \to \infty} \frac{1}{R^2} \int_0^R g(r_{ij}) r_{ij} \, \mathrm{d}r_{ij} = 0 \tag{4}$$

Because of the impossibility of interpenetration of the cylindrical fibers and their independence when they are infinitely apart, function $g(r_{ij})$ satisfies the following conditions:

$$g(r_{ij}) = 1 \quad \text{if } r_{ij} < 2a_n; \qquad \lim_{r_{ij} \to \infty} g(r_{ij}) = 0 \tag{5}$$

The first of these conditions holds for the nonoverlapping sets of cylindrical fibers. The second condition is correct if the correlation in spatial positions of the fibers disappears.

A function satisfying these conditions is expressed as

$$g(r_{ij}) = \begin{cases} 1, & r_{ij} \leq 2a_n \\ \delta \exp(-r_{ij}/L), & r_{ij} > 2a_n \end{cases} \tag{6}$$

where δ $[0 < \delta \leq \exp(2a_n/L)]$ is the correlation coefficient, and $L > 0$ is the correlation length.

IV. Multiple Scattering of Thermal Waves by Fibers and the Wave Fields

Based on the Fourier heat conduction law, the heat conduction equation in composites, in the absence of heat sources, is described as

$$\nabla^2 T(r, t) = \frac{1}{D} \frac{\partial T}{\partial t} \tag{7}$$

where $\nabla^2 = \partial^2/\partial x^2 + \partial^2/\partial y^2$ represents the two-dimensional Laplace operator, T is the temperature in composite materials, and D is the thermal diffusivity with

$$D = \lambda/\rho c \tag{8}$$

The solution of periodic steady state is investigated. Suppose that

$$T = T_0 + \mathrm{Re}[\vartheta \exp(-\bar{i}\omega t)] \tag{9}$$

where T_0 is the average temperature, $\bar{i}$ is the imaginary unit, and ω is the incident frequency of thermal waves.

Substituting Eq. (9) into Eq. (7), the following equation can be obtained:

$$\nabla^2\vartheta + \kappa^2\vartheta = 0 \tag{10}$$

where κ is the wave number of complex variables in composites, and

$$\kappa = (1+\bar{i})k \tag{11}$$

with $k = \sqrt{\omega/2D}$ being the incident wave number.

It is assumed that the thermal waves propagate in the positive x direction. Thus, the incident thermal waves in the matrix are expressed, using wave function expansion method, as

$$\vartheta^{(\mathrm{in})} = \vartheta_0 e^{i(\kappa x-\omega t)} = \vartheta_0 \sum_{m=-\infty}^{\infty} \bar{i}^m J_m(\kappa r) e^{\bar{i}(m\theta-\omega t)} \tag{12}$$

where the superscript (in) stands for the incident waves in the matrix, $J_m(\cdot)$ are the mth Bessel functions of the first kind, and ϑ_0 is the temperature amplitude of incident thermal waves in the matrix. It should be noted that all wave fields have the same time variation $e^{-\bar{i}\omega t}$, which is omitted in all subsequent representations for notational convenience.

When the thermal waves propagate in the fibrous composite material, the waves are scattered by the fibers, and the scattered waves of the fibers are expanded in a series of outgoing Hankel functions. The scattered field around the ith fiber in the matrix is expressed in the form

$$\vartheta_i^{(s)} = \sum_{m=-\infty}^{\infty} A_{im} H_m^{(1)}(\kappa r_i) e^{\bar{i}m\theta_i} \tag{13}$$

where the superscript (s) stands for the scattered waves, $H_m^{(1)}(\cdot)$ are the mth Hankel functions of the first kind, and A_{im} is the mode coefficient that accounts for the distortion of the scattered cylindrical waves by the ith fiber.

Thus, the total scattered field in composites is expressed as

$$\vartheta^{(s)} = \sum_{i=1}^{N} \vartheta_i^{(s)} \tag{14}$$

The total temperature in the matrix ϑ^t should be produced by the superposition of the incident field and the scattered fields of every fiber; that is,

$$\vartheta^t = \vartheta^{(\mathrm{in})} + \vartheta^{(s)} \tag{15}$$

The refracted waves inside the ith fiber are standing waves and can be expressed as

$$\vartheta_i^{(r)} = \sum_{m=-\infty}^{\infty} B_{im} J_n(\kappa_f r_i) e^{\bar{i}m\theta_i} \tag{16}$$

where the superscript (r) stands for the refracted waves, and B_{im} are the mode coefficients of refracted waves.

The temperature in the lth layer ϑ^l of the ith fiber may be described by the sum of the two components (outgoing and ingoing) and is expressed in the following form [21,22]:

$$\vartheta_i^l = \left[\sum_{m=-\infty}^{\infty} E_{im}^l H_m^{(1)}(\kappa_l r_i) e^{\bar{i}m\theta_i} + \sum_{m=-\infty}^{\infty} F_{im}^l H_m^{(2)}(\kappa_l r_i) e^{\bar{i}m\theta_i}\right] \quad (l = 1, 2, \ldots, n) \tag{17}$$

where $H_m^{(2)}(\cdot)$ are the mth Hankel functions of the second kind, and denote the ingoing waves, and E_m^l and F_m^l are the mode coefficients in the lth layer.

The wave numbers κ_l in the lth layer and κ_0 in the cylindrical fiber are given by

$$\kappa_l = (1+\bar{i})\sqrt{\omega/2D_l}, \qquad (l = 1, 2, \ldots, n) \tag{18}$$

$$\kappa_0 = (1+\bar{i})\sqrt{\omega/2D_0} \tag{19}$$

where $D_l = \lambda_l/(\rho_l c_l)$ and $D_0 = \lambda_0/(\rho_0 c_0)$.

V. Boundary Conditions and Solution of Mode Coefficients

The boundary conditions on C_i^n, C_i^l $(l = 1, 2, \ldots, n-1)$, and C_i^0 around the ith fiber are given by

$$\vartheta_i^n = \vartheta^t, \qquad q_{ir}^n = q_r^t \quad \text{for} \quad r_i = a_n \tag{20}$$

$$\vartheta_i^l = \vartheta_i^{l+1}, \quad q_{ir}^l = q_{ir}^{l+1} \quad \text{for} \quad r_i = a_l, \quad (l = 1, 2, \ldots, n-1) \tag{21}$$

$$\vartheta_i^1 = \vartheta_i^{(r)}, \qquad q_{ir}^1 = q_{ir}^{(r)} \quad \text{for} \quad r_i = a_0 \tag{22}$$

where q_{ir} is the heat flow density in the radial direction corresponding to ϑ_i, and

$$q_{ir} = -\lambda_i \frac{\partial\vartheta_i}{\partial r_i}$$

The continuous boundary condition of temperature on C_i^n gives

$$\sum_{m=-\infty}^{\infty} [E_{im}^n H_m^{(1)}(\kappa_n a_n) e^{\bar{i}m\theta_i} + F_{im}^n H_m^{(2)}(\kappa_n a_n)] e^{\bar{i}m\theta_i} = \vartheta_0 e^{\bar{i}\kappa x} + \sum_{j=1}^{N}\sum_{m=-\infty}^{\infty} A_{jm} H_m^{(1)}(\kappa r_j) e^{\bar{i}m\theta_j} \tag{23}$$

Multiplying by $e^{-\bar{i}s\theta_1}$ and integrating from 0 to 2π on both sides of Eq. (23), the following equation can be obtained:

$$H_s^{(1)}(\kappa_n a_n) E_{is}^n + H_s^{(2)}(\kappa_n a_n) F_{is}^n = \vartheta_0 \bar{i}^s J_s(\kappa a_n) e^{\bar{i}\kappa r_{io}\cos\theta_{io}} + \sum_{j=1}^{N}\sum_{m=-\infty}^{\infty} A_{jm} K_{jims} \tag{24}$$

where

$$K_{jims} = \begin{cases} \frac{1}{2\pi}\int_0^{2\pi} [H_m^{(1)}(\kappa a_n) e^{\bar{i}m\theta_j} e^{-\bar{i}s\theta_i}\, \mathrm{d}\theta_i & j \neq i \\ H_s^{(1)}(\kappa a_n)\delta_{ms} & j = i \end{cases} \tag{25}$$

in which δ_{ms} is Kronecker delta function. Using the addition theorem for Hankel functions, one can obtain

$$K_{jims} = \frac{1}{2\pi}\int_0^{2\pi} \left\{ e^{\bar{i}m\theta_{ij}} (-1)^m \sum_{v=-\infty}^{\infty} (-1)^v J_v(\kappa a_n) H_{v-m}^{(1)}(\kappa r_{ij}) e^{\bar{i}v(\theta_i-\theta_{ij})} \right\} e^{-\bar{i}s\theta_i}\, \mathrm{d}\theta_i = J_s(\kappa a_n) H_{m-s}^{(1)}(\kappa r_{ij}) e^{\bar{i}(m-s)\theta_{ij}}, \qquad (j \neq i) \tag{26}$$

where (r_{ij}, θ_{ij}) are the coordinates of o_j referred to o_i as origin.

Then, Eq. (24) is rewritten as

$$H_s^{(1)}(\kappa_n a_n)E_{is}^n + H_s^{(2)}(\kappa_n a_n)F_{is}^n = A_{is}H_s^{(1)}(\kappa a_n) + J_s(\kappa a_n) \times \left[\vartheta_0 \bar{i}^s e^{\bar{i}\kappa r_{io}\cos\theta_{io}} + \sum_{j=1, j\neq i}^{N} \sum_{n=-\infty}^{\infty} A_{j,n+s} H_n^{(1)}(\kappa r_{ij}) e^{\bar{i}n\theta_{ij}}\right] \quad (27)$$

Similarly, the continuous boundary conditions of temperature on C_i^l $(l = 1, 2, \ldots, n-1)$ and C_i^0 give

$$E_{is}^l H_s^{(1)}(\kappa_l a_l) + F_{is}^l H_s^{(2)}(\kappa_l a_l) = E_{is}^{l+1} H_s^{(1)}(\kappa_{l+1} a_{l+1}) + F_{is}^{l+1} H_s^{(2)}(\kappa_{l+1} a_{l+1}) \quad (28)$$

$$B_{is} J_s(\kappa_f a_0) = E_{is}^1 H_s^{(1)}(\kappa_1 a_0) + F_{is}^1 H_s^{(2)}(\kappa_1 a_0) \quad (29)$$

According to the continuous boundary conditions of heat flux density on C_i^n, C_i^l $(l = 1, 2, \ldots, n-1)$ and C_i^0, one can obtain

$$\lambda_n \left[E_{is}^n \frac{\partial}{\partial a_n} H_s^{(1)}(\kappa_n a_n) + F_{is}^n \frac{\partial}{\partial a_n} H_s^{(2)}(\kappa_n a_n)\right] = \lambda \left\{\frac{\partial}{\partial a_n} H_s^{(1)}(\kappa a_n) A_{is} + \frac{\partial}{\partial a_n} J_s(\kappa a_n) \left[\vartheta_0 \bar{i}^s e^{\bar{i}\kappa r_{io}\cos\theta_{io}} + \sum_{j=1, j\neq i}^{N} \sum_{m=-\infty}^{\infty} A_{j,m+s} H_m^{(1)}(\kappa r_{ij}) e^{\bar{i}m\theta_{ij}}\right]\right\} \quad (30)$$

$$\lambda_l \left[E_{is}^l \frac{\partial}{\partial a_l} H_s^{(1)}(\kappa_l a_l) + F_{is}^l \frac{\partial}{\partial a_l} H_s^{(2)}(\kappa_l a_l)\right] = \lambda_{l+1} \left[E_{is}^l \frac{\partial}{\partial a_{l+1}} H_s^{(1)}(\kappa_{l+1} a_{l+1}) + F_{is}^l \frac{\partial}{\partial a_{l+1}} H_s^{(2)}(\kappa_{l+1} a_{l+1})\right]$$

$$\lambda_0 \left[B_s \frac{\partial}{\partial a_0} J_s(\kappa_f a_0)\right] = \lambda_1 \left[E_s \frac{\partial}{\partial a_0} H_s^{(1)}(\kappa_c a_0) + F_s \frac{\partial}{\partial a_0} H_s^{(2)}(\kappa_c a_0)\right] \quad (31)$$

According to Eqs. (23–31), the expanded coefficient of scattered waves A_{is} can be expressed as

$$A_{is} = A_s' T_i^s \quad (32)$$

where

$$A_s' = X_s \frac{H_s^{(1)}(\kappa_c a_n)}{H_s^{(1)}(\kappa a_n)} + Y_s \frac{H_s^{(2)}(\kappa_c a_n)}{H_s^{(1)}(\kappa a_n)} - \frac{J_s^{(1)}(\kappa a_n)}{H_s^{(1)}(\kappa a_n)} \quad (33)$$

$$T_i^s = \vartheta_0 \bar{i}^s e^{\bar{i}\kappa r_{io}\cos\theta_{io}} + \sum_{j=1, j\neq i}^{N} \sum_{n=-\infty}^{\infty} A_{n+s}' T_j^{n+s} H_n^{(1)}(\kappa r_{ij}) e^{\bar{i}n\theta_{ij}} \quad (34)$$

in which X_s and Y_s are shown in the Appendix. It should be noted that T_i^s is the temperature field in any point of composites.

When either o_i or o_i and o_j together are held fixed, to determine the mean temperature field in composites $\langle T_i^s \rangle_i$, the conditional expectation of the fiber distribution is used. From Eq. (34), one can obtain

$$\langle T_i^s \rangle_i = \vartheta_0 \bar{i}^s e^{\bar{i}\kappa r_{io}\cos\theta_{io}} + n_0 \left(1 - \frac{1}{N}\right) \sum_{n=-\infty}^{\infty} A_{n+s}' \times \int_{r_{io}, r_{jo} * S} [1 - g(r_{ij})] \langle T_j^{n+s} \rangle_{ij} H_n^{(1)}(\kappa r_{ij}) e^{\bar{i}n\theta_{ij}} \, d\tau_j \quad (35)$$

where $n_0 = N/S = V_f/(\pi a_0^2)$ is the number of cylindrical fibers per unit area, V_f is the volume fraction of fibers in the matrix, S is the total area of composite materials, and $g(r_{ij})$ shown in Eq. (6) is the pair correlation function of fiber distribution. Equation (35) involves the conditional expectation with two cylindrical fibers held fixed. If we take the conditional expectation of Eq. (35) with two cylindrical inclusions held fixed, the resulting equation will contain the conditional expectation with three cylindrical inclusions held fixed, and so on. To eliminate this hierarchy, Lax's quasi-crystalline approximation theory [19] is applied. In Lax's quasi-crystalline approximation theory [19], the two-inclusion correlation function is involved, and the mean temperature field is expressed as

$$\langle T_i^s \rangle_{ij} = \langle T_i^s \rangle_i, \qquad i \neq j \quad (36)$$

According to the extinction theorem, when S and N become infinitely large, the incident wave is extinguished on entering the composite, and so the corresponding term in Eq. (35) can be dropped. Thus, this equation is simplified to

$$\langle T_i^n \rangle_i = n_0 \sum_{s=-\infty}^{\infty} A_{n+s}' \times \int_{|r_{io} - r_{jo}| > 2a_n} [1 - g(r_{ij})] \langle T_j^{n+s} \rangle_j H_s^{(1)}(\kappa r_{ij}) e^{\bar{i}s\theta_{ij}} \, d\tau_j \quad (37)$$

Assuming the existence of an average plane wave, the solution of Eq. (35) is proposed as

$$\langle T_i^n \rangle_i = \bar{i}^n T_n e^{\bar{i}K r_{io}\cos\theta_{io}} \quad (38)$$

where T_n is a constant, and K is the wave number of the effective thermal waves. Making use of the Green's theorem and wave function expansion method, the following can be obtained:

$$e^{\bar{i}K r_{jo}\cos\theta_{jo}} = e^{\bar{i}K r_{io}\cos\theta_{io}} \sum_{m=-\infty}^{\infty} \bar{i}^{-m} J_m(K r_{ji}) e^{-\bar{i}m\theta_{ji}} \quad (39)$$

The first integral appearing in Eq. (37) can be simplified as

$$\begin{aligned}\int_{|r_{io} - r_{jo}| > 2a_n} & e^{\bar{i}K x_{io}} H_s^{(1)}(\kappa r_{ij}) e^{\bar{i}s\theta_{ij}} \, d\tau_j \\ &= \frac{1}{\kappa^2 - K^2} \int_{|r_{io} - r_{jo}| > 2a_n} [(\nabla^2 e^{\bar{i}K x_{jo}}) H_s^{(1)}(\kappa r_{ij}) e^{\bar{i}s\theta_{ij}} - e^{\bar{i}K x_{jo}} \nabla^2 H_s^{(1)}(\kappa r_{ij}) e^{\bar{i}s\theta_{ij}}] \, d\tau_j \\ &= e^{\bar{i}K x_{io}} \frac{2\pi a_n \bar{i}^{-s}}{\kappa^2 - K^2} \left[J_s(2K a_n) \frac{\partial}{\partial a_n} H_s^{(1)}(2\kappa a_n) - H_s^{(1)}(2\kappa a_n) \frac{\partial}{\partial a_n} J_s(2K a_n)\right]\end{aligned} \quad (40)$$

In the same way, the second integral in Eq. (39) can be also simplified. Then Eq. (37) reduces to the system of equations

$$T_n = 2\pi n_0 \sum_{s=-\infty}^{\infty} A_{n+s}' T_{n+s} \left\{\frac{a_n}{\kappa^2 - K^2} \left[J_s(2K a_n) \frac{\partial}{\partial a_n} H_s^{(1)}(2\kappa a_n) - H_s^{(1)}(2\kappa a_n) \frac{\partial}{\partial a_n} J_s(2K a_n)\right] - \int_{2a_n}^{\infty} g(r_{ij}) J_s(K r_{ij}) H_s^{(1)}(\kappa r_{ij}) r_{ij} \, dr_{ij}\right\} \quad (41)$$

The set of Eqs. (41) consists of an infinite number of homogeneous linear equations determining the coefficients T_n. For a nontrivial solution of T_n, the determinant must vanish, and this leads to the equation for the effective wave number K. It is noted that the effects of multiple scattering on the coherent waves are of great practical importance for the volume fraction of fibers ($V_f = 0.01$–0.5). At very low volume fraction of fibers ($V_f < 0.01$), the multiple scattering effect can be neglected and each fiber can be treated as independent.

The expressions of $J_s(x)$ and $H_s^{(1)}(x)$ are written as

$$J_s(x) = \sum_{k=0}^{\infty} \frac{(-1)^k}{k!(s+k)!} \left(\frac{x}{2}\right)^{s+k}$$
$$H_s^{(1)}(x) = \frac{i}{\sin(s\pi)} [J_s(x) e^{-is\pi} - J_{-s}(x)] \tag{42}$$

When L is sufficiently small compared to the wavelength, by using Eqs. (42), and retaining the lowest order terms for $h/a_0 = 0$, one can obtain

$$T_n \simeq -\pi c \sum_{s=-\infty}^{\infty} A''_{n+s} T_{n+s} \left[\frac{1}{\pi} \left(\frac{K}{\kappa}\right)^s \frac{1}{1-(K/\kappa)^2} + \frac{i}{2} \kappa^2 P_s \right] \tag{43}$$

where

$$A''_0 = \frac{\rho_0}{\rho} - 1, \qquad A''_{\pm 1} = \frac{\lambda - \lambda_0}{\lambda + \lambda_0}, \qquad A''_q = 0, \qquad (|q| \geq 2)$$
$$P_0 \simeq \frac{2i}{\pi} \delta L^2 \left(1 + \log\frac{\kappa L}{2} - \frac{i\pi}{2}\right), \qquad P_{\pm 1} \simeq \frac{i}{\pi} \delta L^2 \frac{K}{\kappa}$$
$$P_{\pm 2} \simeq \frac{i}{2\pi} \delta L^2 \left(\frac{K}{\kappa}\right)^2, \qquad P_v = 0, \qquad |v| \geq 3$$

VI. Nonsteady Effective Properties of the Fiber-Reinforced Composites

According to Eq. (11), the nonsteady effective thermal conductivity λ^{eff} can be easily obtained from the effective propagating wave number as follows:

$$\lambda^{\text{eff}} = \frac{\rho^{\text{eff}} c^{\text{eff}} \lambda}{\rho c} [\text{Re}(k/K)]^2 \tag{44}$$

where Re(•) denotes the real part, and ρ^{eff} and c^{eff} are the effective mass density and effective heat capacity of composites. From [1], it is known that ρ^{eff} and c^{eff} always follow the mixture rule, and $\rho^{\text{eff}} c^{\text{eff}}$ is given by

$$\rho^{\text{eff}} c^{\text{eff}} = \rho c \left\{ 1 - V_f \left(1 + \frac{h}{a_0}\right)^2 \right\} + \rho_0 c_0 V_f + \sum_{l=1}^{n} \frac{h \rho_l c_l V_f}{a_0 n} \left[2 + \frac{h(2l-1)}{n a_0} \right] \tag{45}$$

VII. Numerical Examples and Discussion

To examine the effect of material properties on the nonsteady effective thermal conductivity of composites, A'_s is computed for a given value of k. Next, the complex coefficient matrix M corresponding to T_n in Eq. (41) is formed. The complex determinant of the coefficient matrix is computed using standard Gauss elimination techniques. For a given value of k, the root of the equation $\text{del}(M) = 0$ is searched in the complex plane using Muller's method. Good initial guesses are provided by Eq. (44) at low values of k and these can be used systematically to obtain quick convergence of roots at increasingly higher values of k.

In the following analysis, it is convenient to make the variables dimensionless. To accomplish this step, a representative length scale a_0, where a_0 is the radius of fibers, is introduced. The following dimensionless variables and quantities have been chosen for computation: the incident wave number $k^* = ka_0 = 0.1$–2.0, $h^* = h/a_0 = 0.05$–0.20, $\lambda^* = \lambda_0/\lambda = 2.0$–$8.0$, $c^* = c_0/c = 2.0$–4.0, and $\rho^* = \rho_0/\rho = 2.0$–$4.0$. The dimensionless effective thermal conductivity is $\lambda^e = \lambda^{\text{eff}}/\lambda$.

Specially designed functionally graded interface layers are introduced for a significant improvement of effective thermal conductivity. The character of nonsteady effective thermal conductivity is dependent on the functional form of gradation. In the graded interface layer, the properties are related to the microstructure of two constituents.

Following the work of Sato and Shindo [23], the properties of two special cases of interface material are considered and are given by the following equations.

Case I:

$$P_{\text{I}}(r) = \begin{cases} P_0 & (r_i < a_0) \\ (P - P_0)(\frac{r - a_0}{h}) + P_0 & (a_0 \leq r_i \leq a_0 + h) \\ P & (r_i > a_0 + h) \end{cases} \tag{46}$$

case II:

$$P_{\text{II}}(r) = \begin{cases} P_0 & (r_i < a_0) \\ 4(P - P_0)(\frac{r - (a_0 + h/2)}{h})^3 + \frac{P + P_0}{2} & (a_0 \leq r_i \leq a_0 + h) \\ P & (r_i > a_0 + h) \end{cases} \tag{47}$$

where P denotes the properties (thermal conductivity, specific heat, and density) of composites. In case I, the material properties vary linearly from those of the inclusions to those of the matrix the interface material through the interface material. Case II refers to the case of curvilinear variation of material properties. These two cases are commonly used in engineering. Through comparing the effective thermal conductivity in the two cases, one can obtain the desired thermal behavior by controlling the variation form of the interfacial material properties. The material properties of the layers given above are calculated at midpoint of each layer assuming variations of cases I and II from the boundary of the inclusion to the matrix medium.

The nonsteady effective thermal conductivity of composites as a function of volume fraction of fibers for case I with parameters $k^* = 0.5$, $\lambda^* = 4.0$, $c^* = 2.0$, and $\rho^* = 2.0$ is presented in Fig. 2. It can be seen that the nonsteady effective thermal conductivity increases with the increase of the thickness of the interface. Because the thermal conductivity of the fiber is greater than that of the matrix, the nonsteady effective thermal conductivity increases with the volume fraction of fibers. The effect of the interface on the effective thermal conductivity also increases with the volume fraction of fibers.

The nonsteady effective thermal conductivity of composites as a function of volume fraction of fibers for case I with parameters $k^* = 1.5$, $\lambda^* = 5.0$, $c^* = 2.0$, and $\rho^* = 2.0$ is presented in Fig. 3. It can be seen that the nonsteady effective thermal conductivity decreases with the increase of the thickness of the interface. This phenomenon is due to the multiple scattering of thermal waves that results in the rapid decrease of thermal energy. When the interface thickness is small, the multiple scattering of thermal waves is strong. With the increase of the interface thickness, the multiple scattering of thermal waves becomes weaker. The effect of the interface on the

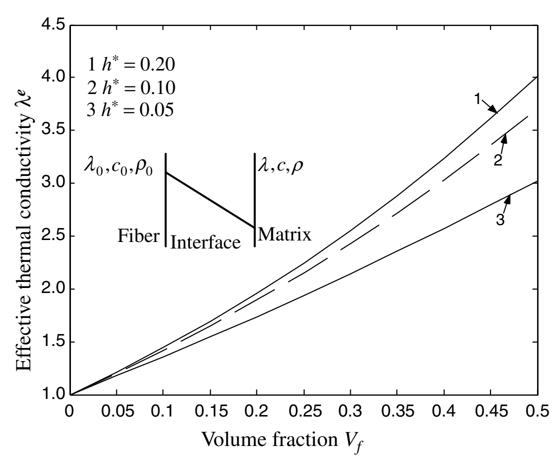

Fig. 2 Nonsteady effective thermal conductivity as a function of volume fraction of fibers with three values of the interface-layer thickness for case I ($k^* = 0.5$, $\lambda^* = 4.0$, $c^* = 2.0$, and $\rho^* = 2.0$).

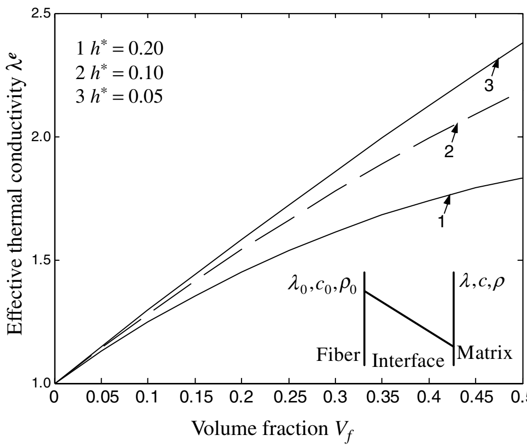

Fig. 3 Nonsteady effective thermal conductivity as a function of volume fraction of fibers for case I ($k^* = 1.5$, $\lambda^* = 5.0$, $c^* = 2.0$, and $\rho^* = 2.0$).

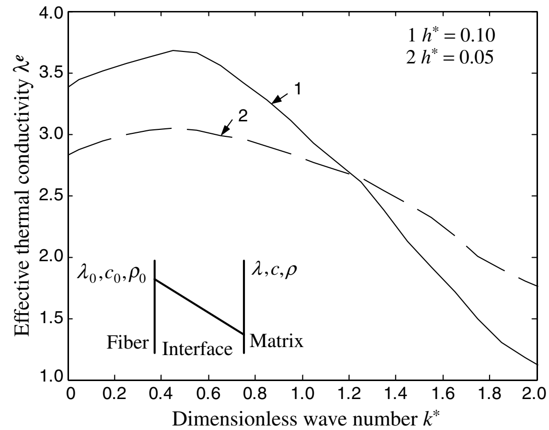

Fig. 5 Nonsteady effective thermal conductivity as a function of dimensionless wave number ($V_f = 0.5$, $\lambda^* = 5.0$, $c^* = 2.0$, and $\rho^* = 2.0$).

effective thermal conductivity also increases with the volume fraction of fibers.

Figure 4 illustrates the nonsteady effective thermal conductivity as a function of dimensionless wave number for case I with parameters $V_f = 0.2$, $\lambda^* = 5.0$, $c^* = 2.0$, and $\rho^* = 2.0$. It can be seen that the nonsteady effective thermal conductivity increases with the increase of dimensionless wave number, then reaches the maximum and decreases as the wave number further increases. In the region of low frequency, the nonsteady effective thermal conductivity increases with the increase of the thickness of the functionally graded layers. However, in the region of high frequency, the nonsteady effective thermal conductivity decreases with the increase of the thickness of the functionally graded layers. The maximum effective thermal conductivity increases with the thickness of the interface. The variation of the nonsteady thermal conductivity with the dimensionless wave number increases with the thickness of the functionally graded layers. The above phenomenon may be caused by the multiple scattering of thermal waves among the distributed fibers with interface. When the wave frequency is lower, the multiple scattering effects do not exist. When the wave frequency is comparable to the fiber size, the multiple scattering effects begin to come into being. In the high-frequency region, the multiple scattering expresses great effect on the effective thermal conductivity.

Figure 5 illustrates the nonsteady effective thermal conductivity as a function of dimensionless wave number for case I with parameters $V_f = 0.5$, $\lambda^* = 5.0$, $c^* = 2.0$, and $\rho^* = 2.0$. Comparing with the results in Fig. 4, it can be seen that the variation of nonsteady effective thermal conductivity with dimensionless wave number increases with the volume fraction of fibers. With the increase of the volume fraction of fibers, the wave number corresponding to the maximum effective thermal conductivity decreases with the volume fraction of fibers. It can be interpreted that the multiple scattering effect increases with the increase of volume fraction of fibers.

The nonsteady effective thermal conductivity of composites as a function of volume fraction of fibers for case II with parameters $k^* = 0.5$, $\lambda^* = 5.0$, $c^* = 2.0$, and $\rho^* = 2.0$ is presented in Fig. 6. It can be seen that the nonsteady effective thermal conductivity increases with the increase of the thickness of the interface. Comparing with the results in Fig. 2, it is clear that the nonsteady thermal conductivity of composites in case I is greater than that in case II. The nonsteady effective thermal conductivity is lower overall and is less sensitive to volume fraction for the functionally graded layer of case II than that for case I.

The nonsteady effective thermal conductivity of composites as a function of volume fraction of fibers for case II with parameters $k^* = 1.5$, $\lambda^* = 5.0$, $c^* = 2.0$, and $\rho^* = 2.0$ is presented in Fig. 7. It can be seen that the nonsteady effective thermal conductivity decreases with the increase of the thickness of the interface. This phenomenon is because the multiple scattering of thermal waves becomes dominant, which results in the rapid attenuation of thermal energy. Comparing with the results in Figs. 2, 3, and 6, it is clear that when the wave frequency increases, the effect of the functionally graded layer on the nonsteady effective thermal conductivity is greater in case II. In the region of low frequency, the multiple scattering is weaker. In the region of high frequency, the effect of the variation form of interface increases with the multiple scattering effects.

Figure 8 illustrates the nonsteady effective thermal conductivity as a function of dimensionless wave number for case II with parameters $V_f = 0.2$, $\lambda^* = 5.0$, $c^* = 2.0$, and $\rho^* = 2.0$. It can be seen that the

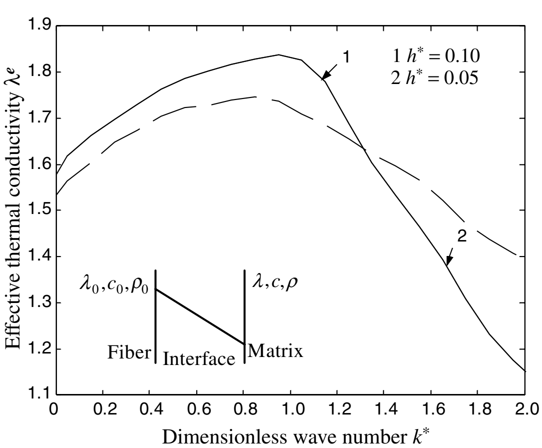

Fig. 4 Nonsteady effective thermal conductivity as a function of dimensionless wave number ($V_f = 0.2$, $\lambda^* = 5.0$, $c^* = 2.0$, and $\rho^* = 2.0$).

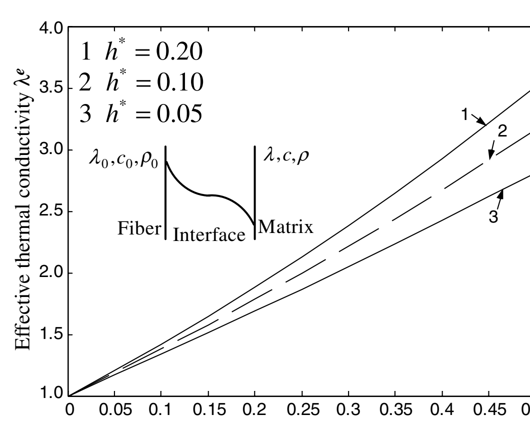

Fig. 6 Nonsteady effective thermal conductivity as a function of volume fraction of fibers ($k^* = 0.5$, $\lambda^* = 5.0$, $c^* = 2.0$, and $\rho^* = 2.0$).

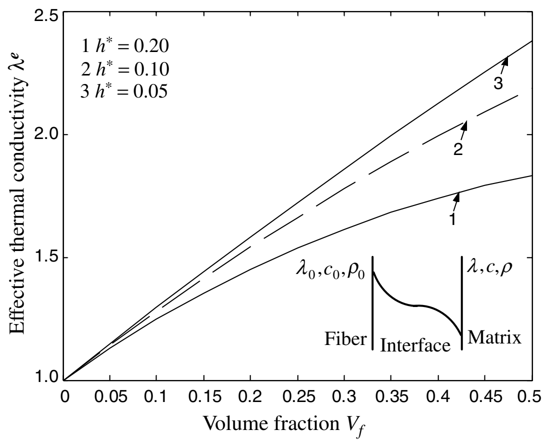

Fig. 7 Nonsteady effective thermal conductivity as a function of volume fraction of fibers ($k^* = 1.5$, $\lambda^* = 5.0$, $c^* = 2.0$, and $\rho^* = 2.0$).

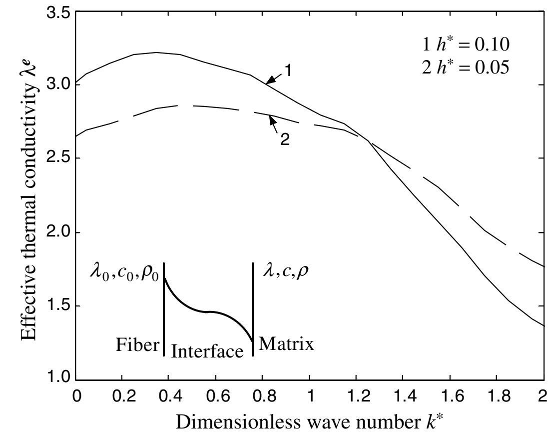

Fig. 9 Nonsteady effective thermal conductivity as a function of dimensionless wave number ($V_f = 0.5$, $\lambda^* = 5.0$, $c^* = 2.0$, and $\rho^* = 2.0$).

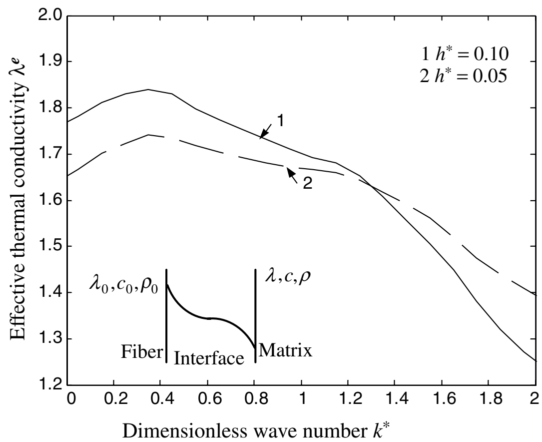

Fig. 8 Nonsteady effective thermal conductivity as a function of dimensionless wave number ($V_f = 0.2$, $\lambda^* = 5.0$, $c^* = 2.0$, and $\rho^* = 2.0$).

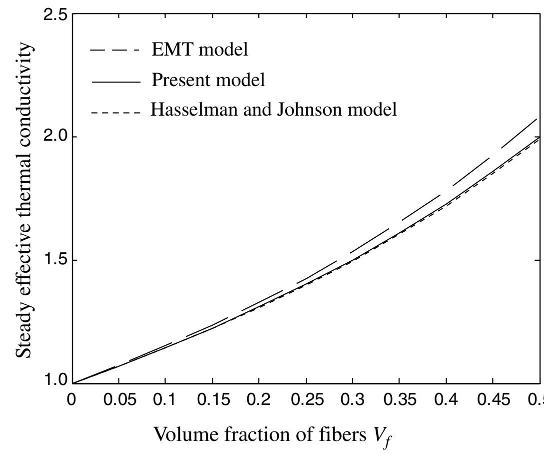

Fig. 10 Comparison of the steady effective thermal conductivity with the effective medium theory model and Hasselman and Johnson [3] ($\lambda_f^* = 5.0$, $c_f^* = 2.0$, $\rho_f^* = 2.0$, $h^* = 0$, and $k^* = 0$).

nonsteady effective thermal conductivity increases with the increase of dimensionless wave number, then reaches the maximum and decreases as wave number further increases. In the region of low frequency, the nonsteady effective thermal conductivity increases with the increase of the thickness of the functionally graded layers. However, in the region of high frequency, the nonsteady effective thermal conductivity decreases with the increase of the thickness of the functionally graded layers. Comparing with the results in Fig. 4, it is clear that the variation of the nonsteady thermal conductivity with the dimensionless wave number is greater in case I than that in case II. The maximum effective thermal conductivity in case II is greater than that in case I. The dimensionless wave number corresponding to the maximum effective thermal conductivity increases is greater in case I than that in case II.

Figure 9 illustrates the nonsteady effective thermal conductivity as a function of dimensionless wave number for case II with parameters $V_f = 0.5$, $\lambda^* = 5.0$, $c^* = 2.0$, and $\rho^* = 2.0$. Comparing with the results in Figs. 4, 8, and 9, it is clear that the variation of the nonsteady thermal conductivity with the dimensionless wave number is greater in case I than that in case II.

Finally, to demonstrate the validity of this dynamical thermal model, the steady effective thermal conductivity of two-phase composites without interface is given. As $k^* \to 0$, the dynamic effective thermal conductivity tends to the steady solutions. In Fig. 10, the results obtained from the present model, Hasselman and Johnson model [3], and effective medium theory model [5] are plotted. Close agreement is seen to exist between the models at low volume fractions; however, the present model predicts a lower value of effective thermal conductivity than the effective medium theory. This is consistent with the criticism of the conventional effective medium theory for overestimating the effective thermal conductivity of two-phase composites when $\lambda_0 > \lambda$. This is attributed to the assumption that the fibers are regarded as the effective medium even at close range.

VIII. Conclusions

The multiple scattering of thermal waves in composites reinforced by dense fibers with functionally graded interfaces is investigated theoretically by employing the wave function expansion method. A semi-analytical solution has been found for the nonsteady effective thermal conductivity of dense fibrous composites. The interactions of temperature field between the fibers in the matrix are considered. Lax's quasi-crystalline approximation is applied to obtain the effective propagating wave number of thermal waves. The analytical solution of the nonsteady effective thermal conductivity of the composite is presented. Comparison with the steady effective thermal conductivity demonstrates the validity of the dynamical thermal model.

In the nonsteady case, the frequency of the thermal waves has great influence on the effective thermal conductivity of composites. In the region of low frequency, the nonsteady effective thermal conductivity increases with the increase of the thickness of the functionally graded layers. However, in the region of high frequency, the nonsteady effective thermal conductivity decreases with the increase of the thickness of the functionally graded layers. The maximum effective thermal conductivity increases with the thickness of interface. The nonsteady effective thermal conductivity is also dependent on the functional form of gradation. Therefore, to obtain desired thermal conductivity, one should choose different thicknesses and functional forms of graded layers under different regions of wave frequency. In addition, the effect of volume fraction of fibers on the multiple scattering and the nonsteady effective thermal conductivity should also be considered.

Appendix: Expressions of X_s and Y_s

The expressions of X_s and Y_s are given by

$$X_s = \frac{P_s K_s^n}{M_s K_s^n - N_s L_s^n}, \qquad Y_s = \frac{-P_s L_s}{M_s K_s - N_s L_s} \tag{A1}$$

where

$$M_s = H_s^{(1)}(\kappa_n a_n)\frac{\partial}{\partial a_n}H_s^{(1)}(\kappa a_n) - \frac{\lambda_n}{\lambda}H_s^{(1)}(\kappa a_n)\frac{\partial}{\partial a_n}H_s^{(1)}(\kappa_n a_n) \tag{A2}$$

$$N_s = H_s^{(2)}(\kappa_n a_n)\frac{\partial}{\partial a_n}H_s^{(1)}(\kappa a_n) - \frac{\lambda_n}{\lambda}H_s^{(1)}(\kappa a_n)\frac{\partial}{\partial a_n}H_s^{(2)}(\kappa_n a_n) \tag{A3}$$

$$P_s = J_s(\kappa a_n)\frac{\partial}{\partial a_n}H_s^{(1)}(\kappa a_n) - H_s^{(1)}(\kappa a_n)\frac{\partial}{\partial a_n}J_s(\kappa_n a_n) \tag{A4}$$

The recurrence formula for L_s^n and K_s^n are expressed as

$$L_s^{l+1} = \frac{L_s^l}{K_s^l}T_s^l + U_s^l, \qquad (l = 1, 2, \ldots, n-1) \tag{A5}$$

$$K_s^{l+1} = \frac{L_s^l}{K_s^l}Q_s^l + V_s^l, \qquad (l = 1, 2, \ldots, n-1) \tag{A6}$$

$$L_s^1 = \frac{\lambda_0}{\lambda_1}H_s^{(1)}(\kappa_1 a_0)\frac{\partial}{\partial a_0}J_s(\kappa_0 a_0) - J_s(\kappa_0 a_0)\frac{\partial}{\partial a_0}H_s^{(1)}(\kappa_1 a_0) \tag{A7}$$

$$K_s = \frac{\lambda_0}{\lambda_1}H_s^{(2)}(\kappa_1 a_0)\frac{\partial}{\partial a_0}J_s(\kappa_0 a_0) - J_s(\kappa_0 a_0)\frac{\partial}{\partial a_0}H_s^{(2)}(\kappa_1 a_0) \tag{A8}$$

In Eqs. (A5) and (A6), T_s^l, Q_s^l, U_s^l, and V_s^l are calculated as

$$T_s^l = \frac{\lambda_{l+1}[H_s^{(2)}(\kappa_l a_l)\frac{\partial}{\partial a_l}H_s^{(1)}(\kappa_{l+1} a_l)] - \lambda_l[H_s^{(1)}(\kappa_{l+1} a_l)\frac{\partial}{\partial a_l}H_s^{(2)}(\kappa_{l+1} a_l)]}{\lambda_l[H_s^{(2)}(\kappa_l a_l)\frac{\partial}{\partial a_l}H_s^{(1)}(\kappa_l a_l) - H_s^{(1)}(\kappa_l a_l)\frac{\partial}{\partial a_l}H_s^{(2)}(\kappa_l a_l)]} \tag{A9}$$

$$Q_s^l = \frac{\lambda_{l+1}[H_s^{(2)}(\kappa_l a_l)\frac{\partial}{\partial a_l}H_s^{(2)}(\kappa_{l+1} a_l)] - \lambda_l[H_s^{(2)}(\kappa_{l+1} a_l)\frac{\partial}{\partial a_l}H_s^{(2)}(\kappa_l a_l)]}{\lambda_l[H_s^{(2)}(\kappa_l a_l)\frac{\partial}{\partial a_l}H_s^{(1)}(\kappa_l a_l) - H_s^{(1)}(\kappa_l a_l)\frac{\partial}{\partial a_l}H_s^{(2)}(\kappa_l a_l)]} \tag{A10}$$

$$U_s^l = \frac{\lambda_{l+1}[H_s^{(1)}(\kappa_l a_l)\frac{\partial}{\partial a_l}H_s^{(1)}(\kappa_{l+1} a_l)] - \lambda_l[H_s^{(1)}(\kappa_{l+1} a_l)\frac{\partial}{\partial a_l}H_s^{(1)}(\kappa_l a_l)]}{\lambda_l[H_s^{(1)}(\kappa_l a_l)\frac{\partial}{\partial a_l}H_s^{(2)}(\kappa_l a_l) - H_s^{(2)}(\kappa_l a_l)\frac{\partial}{\partial a_l}H_s^{(1)}(\kappa_l a_l)]} \tag{A11}$$

$$V_s^l = \frac{\lambda_{l+1}[H_s^{(1)}(\kappa_l a_l)\frac{\partial}{\partial a_l}H_s^{(2)}(\kappa_{l+1} a_l)] - \lambda_l[H_s^{(2)}(\kappa_{l+1} a_l)\frac{\partial}{\partial a_l}H_s^{(1)}(\kappa_l a_l)]}{\lambda_l[H_s^{(1)}(\kappa_l a_l)\frac{\partial}{\partial a_l}H_s^{(2)}(\kappa_l a_l) - H_s^{(2)}(\kappa_l a_l)\frac{\partial}{\partial a_l}H_s^{(1)}(\kappa_l a_l)]} \tag{A12}$$

References

[1] Salazar, A., Terrón, J. M., Sánchez-Lavega, A., and Celorrio, R., "On the Effective Thermal Diffusivity of Fiber-Reinforced Composites," *Applied Physics Letters*, Vol. 80, No. 11, 2002, pp. 1903–1905. doi:10.1063/1.1461422

[2] Maxwell, J. C., *A Treatise on Electricity and Magnetism*, Vol. 1, 3rd ed., Dover, New York, 1954.

[3] Hasselman, D. P. H., and Johnson, L. F., "Interfacial Effect on the Thermal Conductivity of Composites," *Journal of Composite Materials*, Vol. 21, No. 6, 1987, pp. 508–515. doi:10.1177/002199838702100602

[4] Rocha, R. P. A., and Cruz, M. E., "Computation of the Effective Conductivity of Unidirectional Fibrous Composites with an Interfacial Thermal Resistance," *Numerical Heat Transfer, Part A, Applications*, Vol. 39, No. 2, 2001, pp. 179–203. doi:10.1080/104077801300004267

[5] Christon, M., Burns, P. J., and Sommerfeld, R. A., "Quasi-Steady Temperature Gradient Metamorphism in Idealized Dry Snow," *Numerical Heat Transfer, Part A, Applications*, Vol. 25, No. 3, 1994, pp. 259–278. doi:10.1080/10407789408955948

[6] Samantray, P. K., Karthikeyan, P., and Reddy, K. S., "Estimating Effective Thermal Conductivity of Two-Phase Materials," *International Journal of Heat and Mass Transfer*, Vol. 49, Nos. 21–22, 2006, pp. 4209–4219. doi:10.1016/j.ijheatmasstransfer.2006.03.015

[7] Hashin, Z., and Monteiro, P. J. M., "An Inverse Method to Determine the Elastic Properties of the Interphase Between the Aggregate and the Cement Paste," *Cement and Concrete Research*, Vol. 32, No. 8, 2002, pp. 1291–1300. doi:10.1016/S0008-8846(02)00792-5

[8] Kanaun, S. K., and Kudriavtseva, L. T., "Spherically Layered Inclusions in a Homogeneous Elastic Medium," *Journal of Applied Mathematics and Mechanics*, Vol. 50, No. 4, 1986, pp. 483–491. doi:10.1016/0021-8928(86)90013-4

[9] Kanaun, S. K., and Kudriavtseva, L. T., "Elastic and Thermoelastic Characteristics of Composites Reinforced with Unidirectional Fibre Layers," *Applied Mathematics and Mechanics*, Vol. 53, No. 5, 1989, pp. 628–636. doi:10.1016/0021-8928(89)90112-3

[10] Lutz, M. P., and Ferrari, M., "Compression of a Sphere with Radially Varying Elastic Moduli," *Composites Engineering* Vol. 3, No. 9, 1993, pp. 873–884. doi:10.1016/0961-9526(93)90045-L

[11] Lutz, M. P., and Zimmerman, R. W., "Effect of the Interphase Zone on the Bulk Modulus of a Particulate Composite," *Journal of Applied Mechanics* Vol. 63, No. 4, 1996, pp. 855–861. doi:10.1115/1.2787239

[12] Taguchi, T., Igawa, N., Yamada, R., and Jitsukawa, S., "Effect of Thick SiC Interphase Layers on Micro- Structure, Mechanical and Thermal Properties of Reaction-Bonded SiC/SiC Composites," *Journal of Physics and Chemistry of Solids*, Vol. 66, Nos. 2–4, 2005, pp. 576–580. doi:10.1016/j.jpcs.2004.06.034

[13] Sevostianov, I., and Kachanov, M., "Effect Of Interphase Layers on the Overall Elastic and Conductive Properties of Matrix Composites. Applications to Nanosize Inclusion," *International Journal of Solids and Structures*, Vol. 44, Nos. 3–4, 2007, pp. 1304–1315. doi:10.1016/j.ijsolstr.2006.06.020

[14] Monde, M., and Mitsutake, Y., "A New Estimation Method of Thermal Diffusivity Using Analytical Inverse Solution for One-Dimensional Heat Conduction," *International Journal of Heat and Mass Transfer*, Vol. 44, No. 16, 2001, pp. 3169–3177. doi:10.1016/S0017-9310(00)00342-2

[15] Fang, X. Q., Hu, C., and Wang, D. B., "Scattering of Thermal Waves and Nonsteady Effective Thermal Conductivity of Composites with Coated Fibers," *Thermochimica Acta*, Vol. 469, Nos. 1–2, 2008, pp. 109–115. doi:10.1016/j.tca.2008.01.009

[16] Fang, X. Q., "Non-Steady Effective Thermal Conductivity of Matrix Composite Materials with High Volume Concentration of Particles," *Computational Materials Science*, Vol. 44, No. 2, 2008, pp. 481–488. doi:10.1016/j.commatsci.2008.04.008

[17] Fang, X. Q., "Scattering of Thermal Waves and Nonsteady Effective Thermal Conductivity of Unidirectional Fibrous Composites with Functionally Graded Interface," *International Journal of Thermophysics*, Vol. 29, No. 4, 2008, pp. 1439–1456. doi:10.1007/s10765-008-0501-2

[18] Waterman, P. C., and Truell, R., “Multiple Scattering of Waves,” *Journal of Mathematical Physics (Woodbury, New York)* Vol. 2, 1961, pp. 512–537.
doi:10.1063/1.1703737
[19] Lax, M., “Multiple Scattering of Waves, 2. The Effective Field in Dense Systems,” *Physical Review*, Vol. 85, 1952, pp. 621–629.
doi:10.1103/PhysRev.85.621
[20] Nozaki, H., and Shindo, Y., “Effect of Interface Layers on Elastic Wave Propagation in a Fiber-Reinforced Metal-Matrix Composite,” *International Journal of Engineering Science*, Vol. 36, No. 4, 1998, pp. 383–394.
doi:10.1016/S0020-7225(97)00083-9
[21] Sinai, J., and Waag, R. C., “Ultrasonic Scattering by Two Concentric Cylinders,” *Journal of the Acoustical Society of America*, Vol. 83, No. 5, 1988, pp. 1728–1735.
doi:10.1121/1.396505
[22] Joo, Y. S., Ih, J. G., and Choi, M. S., “Inherent Background Coefficients for Acoustic Resonance Scattering from Submerged, Multilayered, Cylindrical Structures,” *Journal of the Acoustical Society of America*, Vol. 103, No. 2, 1998, pp. 900–910.
doi:10.1121/1.421207
[23] Sato, H., and Shindo, Y., “Multiple Scattering of Plane Elastic Waves in a Fiber-Reinforced Composite Medium with Graded Interfacial Layers,” *International Journal of Solids and Structures*, Vol. 38, No. 15, 2001, pp. 2549–2571.
doi:10.1016/S0020-7683(00)00170-0